

METHODS ARTICLE

Bioreactor System to Perfuse Mesentery Microvascular Networks and Study Flow Effects During Angiogenesis

Jessica M. Motherwell, BS,^{1,2} Maximillian Rozenblum,²
Prasad V.G. Katakam, MD, PhD,³ and Walter L. Murfee, PhD²

A challenge for engineering models of angiogenesis is mimicking the physiological complexity of real microvascular networks. Utilizing an alternative top-down tissue culture approach, our laboratory developed the rat mesentery culture model as an *ex vivo* platform for investigating the multicellular dynamics involved during angiogenesis within an intact microvascular network. The objective of this study was to introduce physiologically relevant microvascular perfusion in cultured rat mesentery tissues and demonstrate its effect on angiogenesis. Adult male Wistar rat mesenteric tissues were harvested along with the main feeding artery and vein, and then transferred to a custom-designed biochamber for perfusion. The main feeding artery was cannulated with a 30G needle and secured in place with 7-0 suture. Single-pass perfusion was accomplished using a peristaltic pump in series with the biochamber placed inside an incubator set to standard culture conditions (37°C and 5% CO₂). Flow passed through the vasculature and drained out of the venous side to be collected in a waste reservoir. Tissues were cultured for 48 h with perfusion in the biochamber (Perfused) in serum-supplemented media to stimulate angiogenesis. Control tissues were cultured in biochambers without perfusion (Static). Injection with FITC-albumin through the cannulated artery identified the lumens of vessels across the hierarchy of intact microvascular networks and confirmed successful perfusion. Labeling with BSI-lectin identified endothelial cells along microvascular networks and confirmed perfused tissues undergo angiogenesis after 48 h in culture, characterized by an increase in capillary sprouting. The presence of physiologic levels of capillary fluid velocities and associated shear stresses attenuated the angiogenic response compared to static controls. These results demonstrate the effect of perfusion on angiogenesis and establishes the novelty of the rat mesentery culture model as an experimental platform that incorporates perfusion with real microvascular networks in an *ex vivo* environment.

Keywords: angiogenesis, bioreactor, tissue culture model, shear stress

Impact Statement

Microvascular remodeling, or angiogenesis, plays a central role in multiple pathological conditions, including cancer, diabetes, and ischemia. Tissue-engineered *in vitro* models have emerged as tools to elucidate the mechanisms that drive the angiogenic process. However, a major challenge with model development is recapitulating the physiological complexity of real microvascular networks, including incorporation of the entire vascular tree and hemodynamics. This study establishes a bioreactor system that incorporates real microvascular networks with physiological flow as a novel *ex vivo* tissue culture model, thereby providing a platform to evaluate angiogenesis in a physiologically relevant environment.

Introduction

THE MICROVASCULATURE comprises blood vessels throughout the body that mediate numerous biological functions, including transfer of solutes and waste products, oxygen exchange, and temperature regulation. These microvascular

networks play a central role in both the maintenance of tissue homeostasis and dysfunction associated with multiple pathological conditions, including cancer, diabetes, hypertension, and ischemia.^{1,2}

Consider microvascular growth and remodeling, a process that includes angiogenesis, defined as the growth of new

¹Department of Biomedical Engineering, Tulane University, New Orleans, Louisiana.

²J. Crayton Pruitt Department of Biomedical Engineering, University of Florida, Gainesville, Florida.

³Department of Pharmacology, Tulane University School of Medicine, New Orleans, Louisiana.

blood vessels from existing vasculature. This complex cascade involves the coordination of multiple cell types, intracellular signaling, cell-cell interactions, deposition of extracellular matrix (ECM) proteins, and soluble growth factors.^{3,4} In addition, the cellular dynamics involved are influenced by local mechanical factors. For example, fluid or wall shear stress has been shown to influence endothelial cell proliferation, migration, cytoskeletal reorganization, cell-matrix adhesion, protein phosphorylation, and growth factor production.⁴⁻⁷ Hemodynamic forces can also affect perivascular cell (i.e., pericyte and smooth muscle cell) phenotype and function.^{8,9}

Tissue-engineered *in vitro* models have emerged as tools to elucidate the mechanisms involved during angiogenesis. A challenge with *in vitro* model development is the incorporation of physiological complexity that recapitulates the environment of real tissue. The application of bottom-up tissue engineering approaches, highlighted by cells-in-scaffold models and microfluidic-based systems,¹⁰⁻¹⁵ has successfully incorporated a subset of the important players involved during angiogenesis. For example, microfluidic models have enabled the investigation of shear stress and interstitial flow on endothelial cell migration from lined channels,¹⁵⁻¹⁸ yet whether these effects are characteristic of real microvascular networks remains unknown. Work by Moya *et al.* has demonstrated the ability of microfluidic devices to create perfused capillary networks with endothelial and stromal cells.¹³

More traditional biomaterial-based scaffold methods have successfully incorporated endothelial cells, pericytes, and stromal cells without flow to investigate vessel assembly.¹⁰⁻¹² While these approaches have enabled reductionist studies to focus on specific mechanistic relationships, there remains a gap compared to the *in vivo* environment. This limits our ability to investigate the effects of vessel-specific hemodynamics within real microvascular networks, including functional arterioles, capillaries, and venules.

Alternative tissue-based top-down models for angiogenesis succeed in increasing complexity with incorporating multiple cell types; however, these models have not been fully characterized for physiological relevance and do not incorporate flow in the vasculature. For example, a common *ex vivo* tissue model is the aortic ring assay. While capillary sprouting in this culture system enables the investigation of multiple cell-type interactions (e.g., pericytes, fibroblasts, and endothelial cells), the newly formed vascular structures occur radially from the tissue slice and not from the microvessels where angiogenesis normally occurs.^{19,20} Another tissue culture model for angiogenesis is the retina explant assay.^{21,22} While the retinal *ex vivo* system has been used for time-lapse observation of angiogenesis, the ability to investigate pericyte-endothelial cell interactions and to incorporate vessel perfusion has not been demonstrated. Thus, the same gap associated with the *in vitro* models is left with tissue culture approaches as well.

In an attempt to fill this gap, our laboratory has developed the rat mesentery culture model as an alternative top-down tissue engineering approach. The model takes advantage of rat mesentery, a very thin (20–40 μm) and translucent tissue,²³ that enables imaging of real microvascular networks down to the single cell level without the need for complex microscopy. Importantly, our model includes blood vessels,

lymphatic vessels, endothelial cells, smooth muscle cells, pericytes, interstitial cells, immune cells, and ECM proteins, comprising the structure of branched microvascular networks. The microvascular structures remain intact during culture and can be imaged over the time course of angiogenesis *in vitro*.^{24,25}

We have previously demonstrated that the model can be used to investigate pericyte-endothelial cell interactions during capillary sprouting,²⁴ evaluate the effects of anti-angiogenic drugs,²⁶ and determine the ability of arterioles to constrict during angiogenesis.²⁷ However, for the investigation of the effects of vessel-specific hemodynamics, the incorporation of vessel perfusion is needed. The objective of this study was to introduce physiologically relevant microvascular perfusion in cultured rat mesentery tissue and demonstrate its effect on angiogenesis.

Herein, we report a novel open-loop bioreactor system that enables perfusion of blood microvascular networks and live tissue imaging. The approach uses a “sandwich” method for assembling the bioreactor to keep mesentery tissue flat and facilitate live imaging. Tissues were stimulated to undergo angiogenesis during culture with and without perfusion to evaluate the influences of flow during angiogenesis. Our results suggest that (1) microvascular networks in rat mesentery tissue can be perfused *ex vivo* and maintain perfusion in culture and (2) the presence of flow influences angiogenesis. The bioreactor system developed for this study establishes the rat mesentery tissue culture as a novel *ex vivo* platform that incorporates the complexity of real microvascular networks with hemodynamics.

Materials and Methods

Mesentery bioreactor system overview

To perfuse blood vessels in microvascular networks, we developed a bioreactor system that features (1) freshly harvested mesentery tissue containing microvascular networks, (2) open-loop perfusion through blood vessels entering the feeding arteriole and exiting the draining venule, and (3) a biochamber that enables live tissue imaging (Fig. 1). Mesentery, a highly vascularized thin connective tissue, was harvested from Wistar rats and the feeding arteriole was cannulated (Fig. 1A). The biochamber was designed to secure the cannulated mesentery tissue flat and enable live imaging during culture (Fig. 1B). The bioreactor system is open loop where the main feeding arteriole of the mesentery tissue is cannulated and fluid is allowed to flow through the vasculature and exit out the draining venule. Flow is generated by a peristaltic pump from the perfusate reservoir and passes through the vasculature, and exits into the waste reservoir (Fig. 1C).

Bioreactor design and fabrication

The mesentery biochamber was fabricated using clear cast acrylic (McMaster Carr, Elmhurst, IL) with laser cutting techniques (Epilog Helix 24, 50-watt CO₂ laser system) to generate designed acrylic structures. The acrylic top and base were designed using Solidworks 3D CAD software (Solidworks, Waltham, MA). Threading was etched into the laser cut holes of the biochamber base and 316 stainless steel-threaded rods (McMaster Carr) were inserted. Polydimethylsiloxane (PDMS) structures were generated by

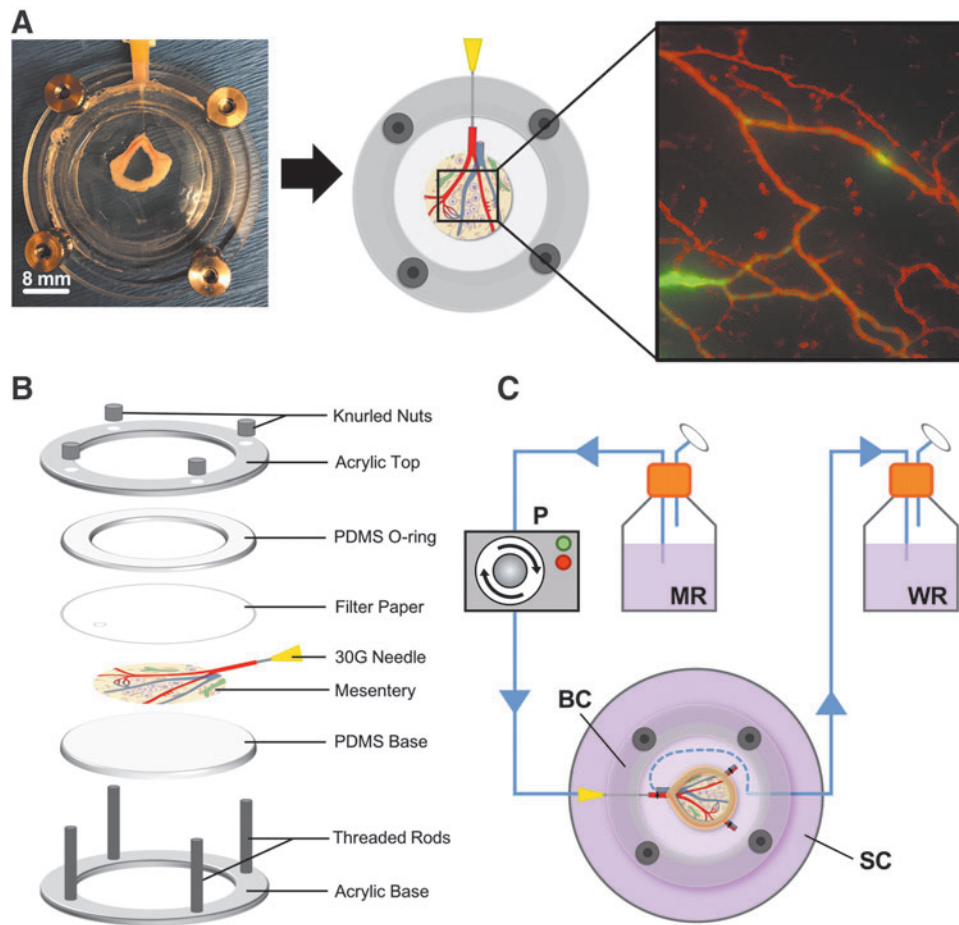


FIG. 1. Bioreactor system for perfused microvascular studies. **(A)** Side-by-side comparison of photographed and illustrated cannulated mesentery tissue secured in the biochamber. **(B)** Expanded view of the assembled biochamber with cannulated mesentery tissue. The chamber is assembled in a “sandwich” manner to hold the tissue flat and enable real-time imaging of microvascular networks. **(C)** Diagram of the open-loop bioreactor system used for *ex vivo* mesentery perfusion studies. Flow is generated by the peristaltic pump and originates from the medium reservoir and enters the cannulated feeding arteriole of the mesentery, circulates through the microvascular network, exits the feeding venule of the mesentery into the biochamber, and drains through the secondary culture dish into the waste reservoir. The blue dashed line in the biochamber depicts media exiting the feeding venule and draining through the secondary culture dish. MR = medium reservoir, WR, waste reservoir; P, pump; BC, biochamber; SC, secondary culture dish.

mixing silicon elastomer base and curing agent (Ellsworth Adhesives, Germantown, WI) at a ratio of 10:1, degassing in a vacuum chamber, and curing for 72 h at room temperature in molds to form patterns. L/S13 tubing (Cole-Parmer, Vernon Hills, IL), which has an inner diameter of 0.8 mm, was used throughout the bioreactor with complimenting luer connectors (Cole-Parmer) of the same dimensions. Three hundred sixteen stainless steel knurled nuts (McMaster Carr) were used to seal the biochamber after assembly and tissue cannulation (Fig. 1B). The biochamber and all bioreactor parts were autoclaved before experimental usage.

Mesentery tissue harvest

All animal experiments were approved by University of Florida’s Institutional Animal and Care Use Committee (protocol 201710060). Adult male Wistar rats (350–400 g) were anesthetized by an intramuscular injection with ketamine (80 mg/kg body weight) and xylazine (8 mg/kg body weight). After confirming the effect of anesthesia, an intraperitoneal injection of heparinized saline (28 mg/kg body

weight) was administered and allowed to circulate for 10 min followed by euthanasia by intracardiac injection of 0.2 mL beuthanasia. Mesentery windows, defined as the translucent connective tissue between artery/vein pairs feeding the small intestine, were aseptically exteriorized onto a custom PDMS stage. Two vascularized mesentery windows were identified and harvested, keeping the feeding artery/vein pair intact; marginal vessels at the base of the tissue were ligated with 7–0 silk sutures (Ethicon, Somerville, NJ) (Fig. 1C). Tissues were immediately rinsed in sterile phosphate-buffered saline (PBS; Gibco, Grand Island, NY) with CaCl_2 and MgCl_2 at 37°C and immersed in sterile minimum essential media (MEM; Gibco) containing 1% Penicillin-Streptomycin (PS; Gibco).

Bioreactor assembly with mesentery tissue

The bioreactor assembly was designed as an open-loop system where media flows from the medium reservoir into the cannulated feeding arteriole of the mesentery tissue, circulates through the microvascular network, exits through

the feeding venule into the biochamber, drains into the secondary culture dish, and finally collects in the waste reservoir (Fig. 1C). Bioreactor tubing was connected to a peristaltic pump (Living Systems, St. Albans City, VT) and three-way stopcock. Biochambers were assembled by first placing the PDMS base between the threaded rods of the acrylic biochamber base. Harvested mesentery tissues were then transferred to the biochamber and the feeding arteriole was cannulated with a 30G needle connected to bioreactor tubing. Residual blood was removed from microvascular networks in the mesentery tissue by perfusing ~3 mL of heparinized PBS (3 mg/mL). Once the microvascular effluence was clear, the mesentery tissue was covered with a filter membrane (Millipore, Burlington, MA) to keep the tissue flat during culture, followed by adding the PDMS O-ring and acrylic top. The biochamber components were secured together with knurled nuts and 5 mL of medium was added to the well of the chamber to submerge the tissue. The biochamber assembly was then transferred to a secondary culture dish to seal the system. Approximately 250 mL of medium was added to the medium reservoir and the biochamber was connected to the bioreactor tubing and transferred to an incubator for perfusion culture.

Albumin perfusion of microvascular networks

Perfusion in cannulated microvascular networks was assessed in freshly harvested tissues ($t=0$ h) and perfusion-cultured tissues ($t=48$ h). Mesentery tissues were topically labeled with Alexa-Fluor™ 594-conjugated lectin (1:100; Invitrogen, Carlsbad, CA) to visualize microvascular networks. A solution of FITC-conjugated albumin (Sigma-Aldrich, St. Louis, MO) was prepared in PBS (1 mg/mL) and perfused through the cannulated artery. Images were taken before and during perfusion with a 4× and 10× objective from an inverted microscope Olympus IX71 paired with a Photometrics CoolSNAP EZ camera.

Flow experiments

Flow was produced in the microvascular networks using a peristaltic pump set to a rate of 0.12 mL/min. Velocity measurements were obtained by adding 1 μm polystyrene FITC-fluorescent microspheres (Invitrogen) to the perfusate and measuring the distance they traveled through capillary vessels. Videos were captured at a rate of 1 frame per second with a 10× objective from an inverted microscope Olympus IX71 paired with a Photometrics CoolSNAP EZ camera. ImageJ was used to measure the distance microspheres traveled through capillary vessels using the following equation:

$$v = L/t$$

where L is the length the microsphere traveled and t is the elapsed time for the sphere to travel the measured distance. The mean wall shear stress for perfused capillaries was calculated from measured velocities assuming Hagen-Poiseuille flow in a cylindrical pipe:

$$\tau = 8\mu v/D$$

where τ is the wall shear stress, μ is viscosity of the perfusate, v is the measured velocity, and D is the average diameter of the vessel.

Angiogenesis perfusion culture

To examine the effects of flow during angiogenesis, the culture medium was supplemented with 10% fetal bovine serum (FBS; Gibco). Serum was chosen for this study because it produces a robust angiogenic response in mesentery tissues, as demonstrated in our previous publications.^{26,28} Tissues were harvested from adult male Wistar rats and divided into two experimental groups: (1) Static: $n=7$ microvascular networks from three tissues and (2) Perfused: $n=9$ microvascular networks from six tissues. For the Static group, tissues were harvested, cannulated, and secured in the biochamber with 5 mL of medium, and cultured without perfusion with medium changed at 24 h. We added 5 mL of medium to the biochamber in the Static group based on our previous experiments with static culture of mesentery tissue in six-well plates.^{24,25} For the Perfused group, tissues were harvested, cannulated, secured in the biochamber, and cultured with perfusion at a flow rate of 0.12 mL/min. Both experimental groups were cultured in standard culture conditions (5% CO₂ and 37°C) with medium supplemented with 10% FBS for 48 h. After 48 h in culture, tissues were perfused with FITC-conjugated albumin diluted in PBS (1 mg/mL) to ensure microvascular networks maintained flow during culture.

Quantification of angiogenesis

Vascular density and capillary sprouts were quantified from randomly selected microvascular networks per tissue from 10× montage images for the Static, Perfused, and Unstimulated experimental groups. Lectin labeling identified all blood and lymphatic vessels, and blood vessels were distinguished based on their morphology and network structure. Microvascular networks were defined as lectin-positive blood vessel structures having a feeding arteriole, draining venule, and capillary plexus within the translucent window of each mesentery tissue. Vascular density was quantified as the number of lectin-positive blood vessel segments (defined as vascular tubes between two connecting nodes) divided by vascular area (defined as the area of tissue covered by the microvascular network). Capillary sprouts were quantified as the number of lectin-positive blood vessel segments with blind-ended tips divided by vascular area. The mean percentage of vessel-specific sprouts per the total number of sprouts was quantified for arterioles, venules, and capillaries, distinguished based on their morphology and location within the microvascular network.

Capillary sprouts were further divided into two categories, invading or introverting, based on their location within the microvascular networks, similar to previous descriptions of capillary phenotypes during angiogenesis.²⁹ Introverting sprouts were defined as capillary sprouts enclosed within the microvascular network that increase the vascular density of the tissue region. Invading sprouts were defined as capillary sprouts entering the avascular space surrounding the microvascular network, which advances the vasculature into the avascular tissue region. Quantification of angiogenesis was analyzed for the following groups: (1) Static: $n=7$ microvascular networks from three tissues and (2) Perfused: $n=9$ microvascular networks from six tissues. Analysis was performed using the Cell Counter plugin with NIH Fiji open-source software version 2.0.0.³⁰

Immunostaining

Following perfusion culture experiments, mesentery tissues were removed from the biochambers and fixed in 100% methanol at -20°C for 30 min. Tissues were then washed three times in PBS with 0.1% saponin for 10 min each, followed by antibody labeling. Microvascular networks were visualized with Alexa-Fluor 647-conjugated lectin (1:100; Invitrogen) and smooth muscle cells were stained with αSMA Cy3-conjugated primary antibody (1:200; Sigma-Aldrich). Additional tissues were labeled for endothelial cells and vascular pericytes by tagging with CD31 (1:200; BD Pharmingen, San Jose, CA) and NG2 (1:100; Millipore) primary antibodies, followed by streptavidin Cy2-conjugated (1:500; Jackson ImmunoResearch, West Grove, PA) and goat anti-rabbit Cy3-conjugated (1:100; Jackson ImmunoResearch) secondary antibodies. All antibodies were diluted in antibody buffer solution (PBS +0.1% saponin +2% bovine serum albumin +5% normal goat serum). Tissues were washed three times in PBS with 0.1% saponin for 10 min each between primary and secondary antibody labeling incubations.

Image acquisition

Fixed tissues immunolabeled for endothelial cells (CD31) and perivascular cells (αSMA and NG2) were imaged using a 20X (oil, NA=1.4) objective coupled with a $1.5\times$ mag-

nification. For quantification of angiogenesis, tissues labeled for lectin were imaged using a $10\times$ (dry, NA=0.3) objective and montaged with NIS Elements software. All images were acquired on an inverted microscope Olympus IX71 paired with a Photometrics CoolSNAP EZ camera.

Statistical analysis

Data are presented as mean \pm standard deviation (SD). One-way analysis of variance (ANOVA) followed by pairwise comparisons with Tukey's *post hoc* test was used to compare vascular density, total capillary sprouts, and vessel-specific sprouts. Two-tailed Student's *t*-test was used to compare invasive and introverting sprouts as a percent of total sprouts. A *p*-value <0.05 was considered statistically significant and all analysis was performed using GraphPad Prism version 8.0 software.

Results

Demonstration of blood vessel perfusion in cultured microvascular networks

Perfusion in freshly harvested mesentery tissue ($t=0$ h) was confirmed by the presence of FITC-albumin in blood vessel lumens (Fig. 2). Topical labeling with Alexa-594 lectin visualized microvascular networks where arterioles, venules, and capillaries were identified based on morphology

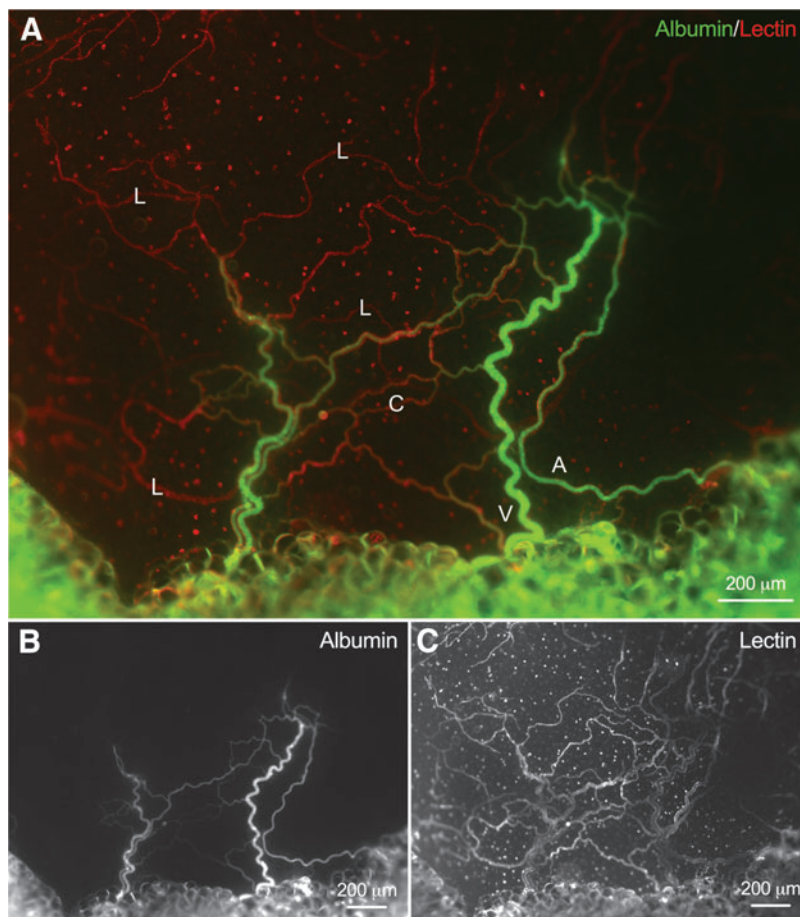


FIG. 2. Demonstration of perfused microvascular networks from freshly harvested mesentery tissue ($t=0$ h). (A) Representative epifluorescence images of microvascular networks perfused with FITC-conjugated albumin (B). (C) Lectin labeling identified microvascular networks where blood and lymphatic vessels were distinguished based on their morphology and network structure. L, lymphatic vessel; V, venule; A, arteriole; C, capillary.

and network structure (Fig. 2C). Albumin was not detected in lymphatic vessels for all perfused tissues (Fig. 2A).

To measure the observed flow in capillaries of perfused microvascular networks, fluorescent microspheres (1 μm diameter) were introduced into blood vessels through the cannulated arteriole. Microspheres were observed across the hierarchy of perfused microvascular networks, including arterioles, venules, and capillaries (Fig. 3A, B and Supplementary Movie S1). Microspheres were tracked as they traveled along the length of perfused capillaries and average velocities were measured (Fig. 3C and Supplementary Movie S2). Capillary microsphere velocities ranged from 0.1 mm/s up to 2.9 mm/s. The mean wall shear stress for perfused capillaries was calculated assuming Hagen-Poiseuille flow in a cylindrical pipe and an approximate fluid viscosity of 0.006922 dyne-s/cm. The mean velocity and shear stress for all observed capillaries ($n=28$ capillaries from four tissues) were 0.9 ± 0.6 mm/s and 8.9 ± 6.9 dyne-s/cm, respectively (Fig. 3C).

In addition, a Spearman's correlation was run to determine the relationship between velocity and shear stress to capillary diameter (Supplementary Fig. S1). There was no significant ($p=0.2887$) correlation between measured velocities to capillary diameter ($r_s=-0.1100$, $n=28$ capillaries). However, there was a moderate, negative monotonic correlation between calculated shear stress to capillary diameter ($r_s=-0.1404$, $p=0.0150$, $n=28$ capillaries).

Injection of FITC-albumin confirmed blood vessels remain perfused after 48 h in culture with the bioreactor system (Fig. 4). Albumin was observed in 9 out of the 10 cultured microvascular networks, including arterioles, venules, and capillaries. Albumin was also observed in network regions characterized by high vessel density, the

presence of blind-ended sprouts, and vascular loops (Fig. 4). Importantly, these characteristics are associated with angiogenesis in rat mesenteric tissues.^{24,28} A subset of capillaries (Fig. 4A, B) and capillary sprouts (Fig. 4C–F) displayed “hot spots” of albumin leakage, indicative of increased permeability.

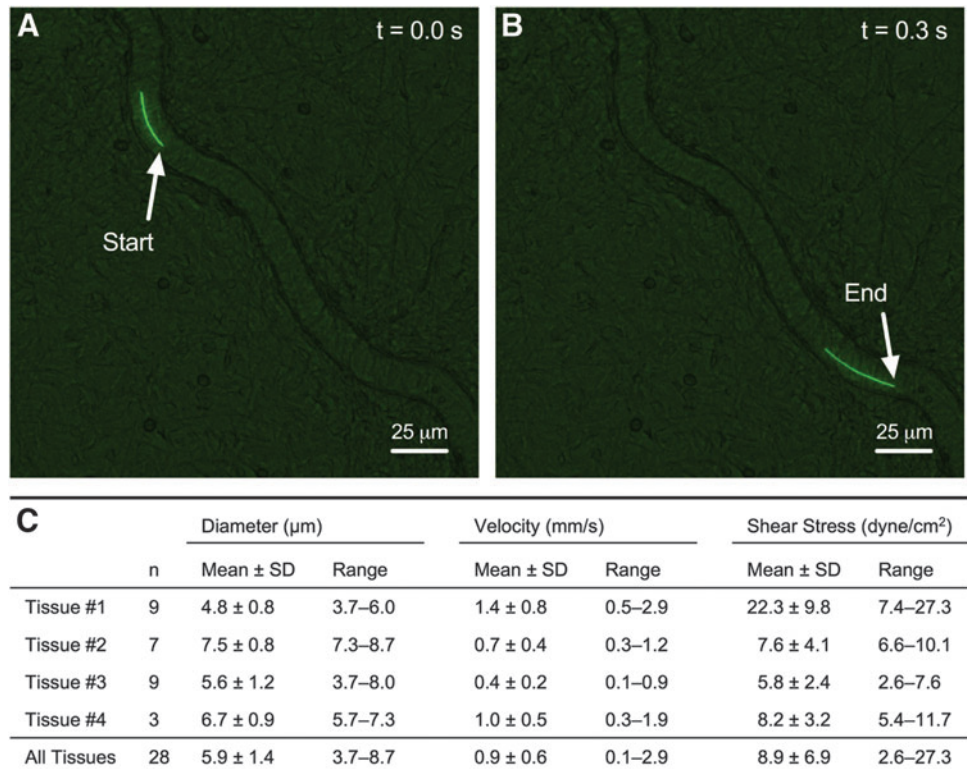
αSMA and NG2 labeling of microvascular networks cultured with perfusion for 48 h identified smooth muscle cells and pericytes, respectively (Fig. 5). Smooth muscle cells were consistently observed to remain tightly wrapped along arterioles and venules (Fig. 5A), and NG2-positive pericytes were observed to wrap along capillaries (Fig. 5B). Injection of FITC-albumin in microvascular networks before tissue fixation confirmed that perfused capillaries and sprouts have perivascular cell coverage (Supplementary Fig. S2).

Presence of perfusion influences angiogenesis

Lectin labeling of mesentery tissues from freshly harvested tissues (Unstimulated) and cultured (Perfused and Static) experimental groups identified endothelial cells along blood vessels in microvascular networks (Fig. 6A–C). Microvascular networks cultured with (Perfused) and without (Static) perfusion underwent angiogenesis, supported by an increase in vascular density and capillary sprouting compared to tissues from the Unstimulated group (vascular density: 26.6 ± 20.7 segments/vascular area, $n=9$; capillary sprouts: 2.4 ± 1.6 sprouts/vascular area, $n=9$).

Qualitative observations of denser microvascular networks were identified in the Static culture group compared to the Perfused culture group, suggesting that the presence of flow in blood vessels influences the density of angiogenic networks. Quantitative analysis of blood endothelial

FIG. 3. Velocity measurements in perfused microvascular networks *ex vivo*. Velocities were calculated by tracking fluorescent microbeads (1 μm diameter) flowing through capillary networks. Example images of the start (A) and end (B) of tracking a microbead along the path of a perfused capillary vessel over the time course of 0.3 s. (C) Velocities and wall shear stresses calculated from capillary vessels across four microvascular networks are shown in the table. Real-time imaging of microspheres traveling through capillaries is shown in Supplementary Movie S1 and visualization of whole network perfusion with microbeads is shown in Supplementary Movie S2.



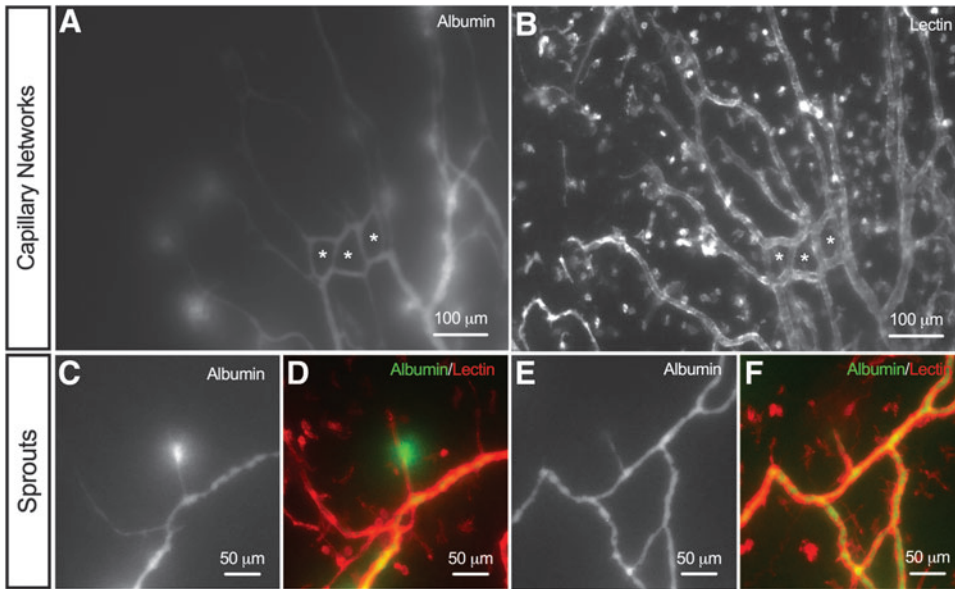


FIG. 4. Microvascular networks maintain perfusion during culture. (A, B) Representative immunofluorescence images of capillary networks perfused with FITC-conjugated albumin (green) after 48 h in culture. The * symbol indicates newly formed capillary loops with perfusion culture. (C–F) Examples of newly formed capillary sprouts perfused with FITC-conjugated albumin (green). Microvascular networks were identified by lectin (red) labeling, where blood and lymphatic vessels were distinguished based on their morphology and network structure.

segments from perfusion-cultured microvascular networks (94.9 ± 44.2 segments/vascular area, $n=9$) revealed a significant decrease ($p=0.0027$) in vascular density compared to static-cultured networks (332 ± 192 segments/vascular area, $n=7$) (Fig. 6C). The number of capillary

sprouts per vascular density between Perfused (28.8 ± 10.6 sprouts/vascular area, $n=9$) and Static (28.3 ± 8.81 sprouts/vascular area, $n=7$) microvascular networks was not significantly different ($p=0.9269$) between experimental groups (Fig. 6D).

Since microvascular density temporally follows capillary sprouting during angiogenesis, the increased density for static networks suggests that the tissues experience an increased rate of microvascular growth. Additional studies compared vascular density in tissues cultured with flow in the biochamber, but without flow in the microvascular networks (Media Sham) to elucidate the effect of medium exchange on angiogenesis (Supplementary Fig. S3). Quantitative analysis revealed a significant decrease ($p=0.0030$) in vascular density from the Perfused group compared to the Media Sham group, suggesting medium exchange alone does not decrease the rate of microvascular growth.

While the total number of capillary sprouts per vascular area was not significantly different between Perfused and Static experimental groups at 48 h ($p=0.9269$), evaluation of vessel-specific sprouts identified differences in sprout location within the network. The mean percentage of sprouts originating from arterioles ($0.7\% \pm 0.3\%$), venules ($2.6\% \pm 1.0\%$), and capillaries ($96.7\% \pm 1.1\%$) was quantified from the total number of sprouts per microvascular network ($n=9$) in the Perfused experimental group. Sprouts originating from arterioles and venules were significantly less ($p<0.0001$) than sprouts originating from capillaries (Fig. 7). Additional analysis of the arteriovenous origin of capillary sprouts revealed no significant difference ($p=0.1252$) in sprouts originating from arterioles versus venules in microvascular networks from the Perfused experimental group (Supplementary Fig. S4).

Capillary sprout phenotype analysis identified differences in both invasive and introverting sprouts in microvascular networks from the Perfused (Fig. 8A) and Static (Fig. 8B) experimental groups. Quantitative evaluation of the percent invasive sprouts per total capillary sprouts identified a significant increase ($p=0.0298$) in microvascular networks cultured with perfusion ($29.5\% \pm 11.0\%$, $n=9$) compared to

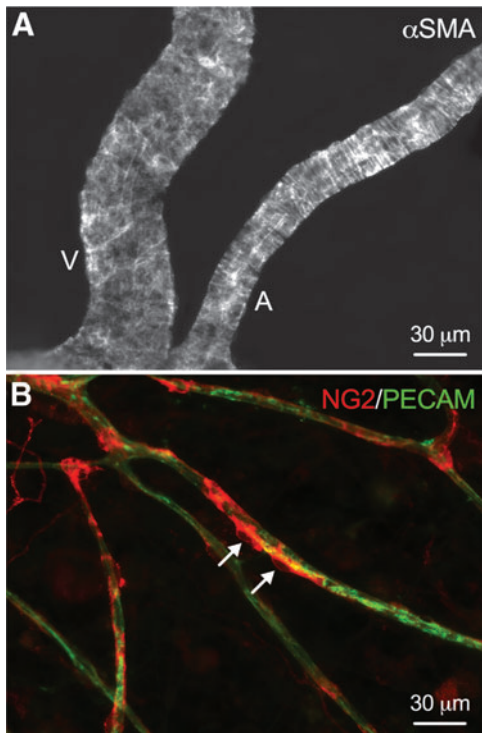


FIG. 5. Representative immunofluorescence images of perivascular cells after 48 h in perfusion culture. (A) α SMA-positive smooth muscle cells maintain tight wrapping morphologies along main arteriole and venule blood vessels in perfused microvascular networks. V, venule; A, arteriole. (B) NG2-positive (red) vascular pericytes maintain close wrapping along blood capillaries (green) in perfused microvascular networks. Arrows indicate individual vascular pericyte cell bodies.

FIG. 6. Evaluation of angiogenesis in microvascular networks cultured with flow (Perfused) and without flow (Static). Microvascular networks from both experimental Perfused (B) and Static (C) groups became angiogenic after 48 h in culture, defined by an increase in vascular density (D) and capillary sprouts (E) compared to microvascular networks from freshly harvested mesentery tissue in the Unstimulated (A) group ($t=0$ h). Angiogenic microvascular networks cultured without flow exhibited significantly ($p=0.0027$) denser vascular structures compared to networks cultured with flow. Interestingly, no significant difference ($p=0.9269$) was observed in capillary sprouting between Perfused and Static groups. *Black, white, and striped bars* represent Unstimulated, Perfused, and Static groups, respectively. The *** and **** indicate a significant difference of $p<0.001$ and $p<0.0001$ by one-way ANOVA and Tukey's *post hoc* method comparing vascular density between Perfused and Static groups. The "ns" indicates no significant difference ($p>0.05$) comparing capillary sprouts between Perfused and Static groups.

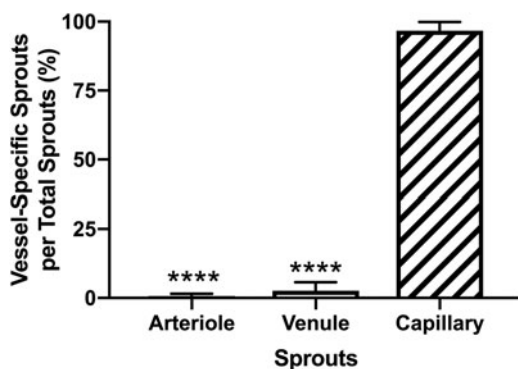
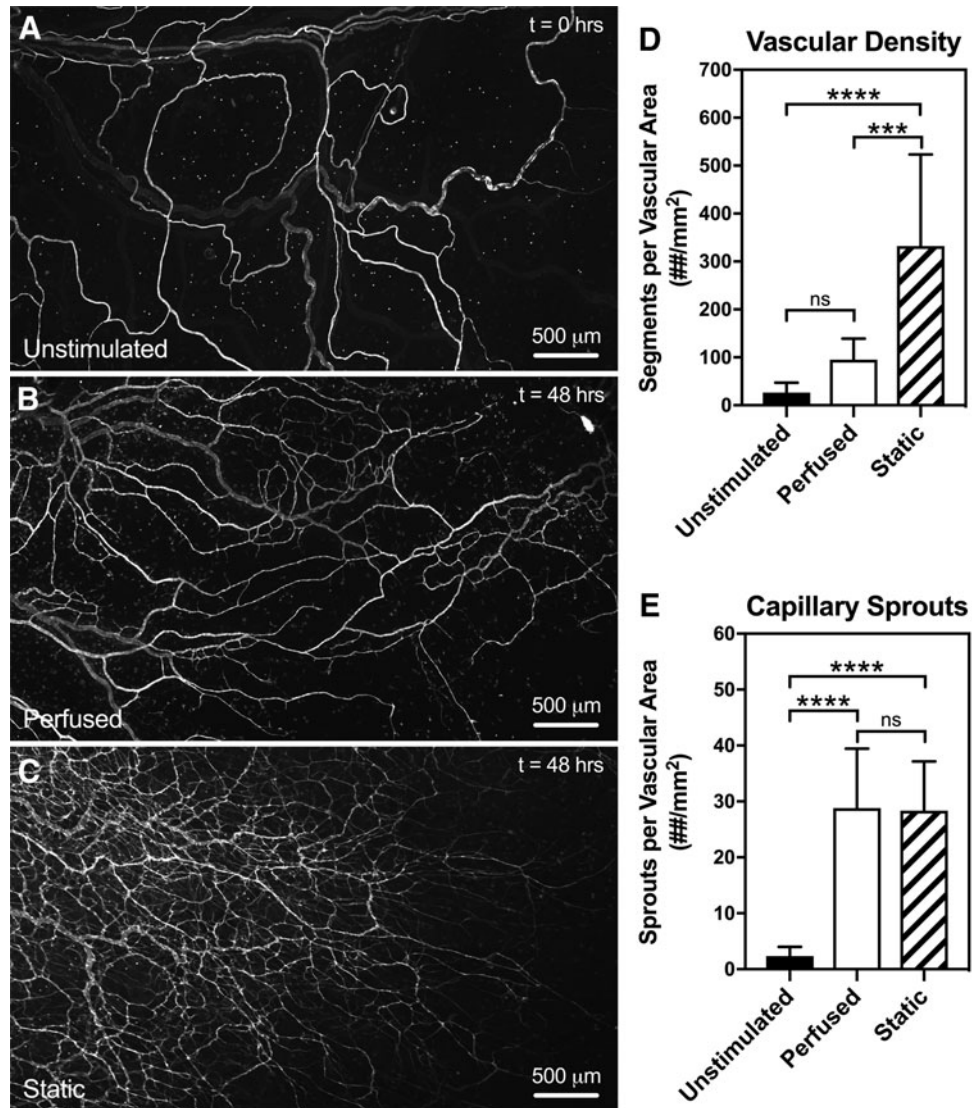


FIG. 7. Evaluation of vessel-specific sprouts as a percentage of total sprouts from cultured tissues in the Perfused experimental group. *Black, white, and striped bars* represent Arteriole Sprouts, Venule Sprouts, and Capillary Sprouts, respectively. The **** indicates a significant difference of $p<0.0001$ by one-way ANOVA and Tukey's *post hoc* method.

static culture ($17.1\% \pm 8.83\%$, $n=7$) (Fig. 8C). In addition, quantitative analysis of the percent introverting sprouts per total capillary sprouts identified a significant decrease ($p=0.0298$) in the Perfused group ($70.5\% \pm 11.0\%$, $n=9$) compared to the Static group ($82.9\% \pm 8.83\%$, $n=7$) (Fig. 8D).

Discussion

The main contribution of this study is the establishment of a novel experimental platform that integrates intact real microvascular networks with physiological vascular perfusion in a bioreactor system to evaluate the effects of flow during angiogenesis. A major challenge for tissue engineering experimental models is matching the complexity of real tissues with physiological flow in an *in vitro* setting.

More recently, advancements in cutting-edge technologies such as microfluidics have helped bridge this gap. For example, Moya *et al.* demonstrated the development of vascularized microtissues that anastomose with side channels to enable the evaluation of flow and shear rates in human capillary networks.¹³ Osaki *et al.* engineered microchannels that mimic the cooperative effects of sprouting

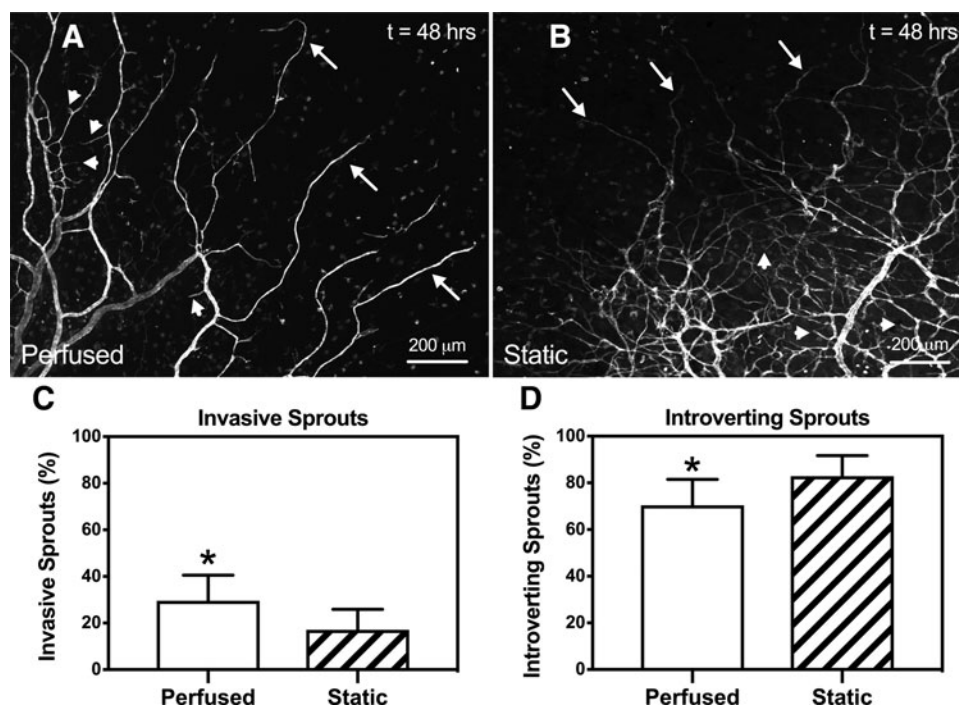


FIG. 8. Quantification of capillary sprout phenotypes. Representative images of both invasive and introverting capillary sprout phenotypes from microvascular networks in the Perfused (A) and Static (B) experimental groups. The *arrows* indicate invasive sprouts and the *arrowheads* indicate introverting sprouts. (C, D) Numbers on x-axis refer to the percent invasive or introverting sprouts per total sprouts for each experimental group. Comparison between Perfused and Static groups revealed a significant increase ($p=0.0298$) in the percent of invasive sprouts in microvascular networks cultured with perfusion. Likewise, a significant decrease ($p=0.0298$) in the percent of introverting sprouts in microvascular networks cultured with perfusion was observed. *White* and *striped bars* represent Perfused and Static groups, respectively. The * indicates a significant difference of $p<0.01$ by two-tailed Student's *t*-test.

interactions during angiogenesis and lymphangiogenesis to elucidate mechanisms of action that drive cancer metastasis and corneal implant rejection.¹⁴ The results of this study establish the physiologic relevance of our bioreactor model as we demonstrate that the presence of flow influences the spatial patterning of angiogenic microvascular networks.

To incorporate perfusion into microvascular networks of mesentery tissue, we introduced flow through a cannulated feeding arteriole secured within a bioreactor system using PDMS and acrylic that was designed, fabricated, and characterized (Fig. 1). Our perfused bioreactor system, inspired by an *ex vivo* lymphatic vessel explant chamber,³¹ enables the following: (1) velocity measurements in physiologically relevant microvascular networks, (2) observation of angiogenesis at specific locations within a vascular tree, and (3) evaluation of wall shear stress on capillary sprouting. The novelty of the perfused mesentery bioreactor system is the incorporation of physiological flow with real microvascular networks in an *ex vivo* environment to study flow effects during angiogenesis.

To create a realistic *in vitro* microvascular model with physiologically relevant flow, perfusion of the vascular networks is required. In this study, perfusion of freshly harvested microvascular networks was demonstrated by injection with FITC-albumin following a vascular flush with heparinized PBS to remove blood (Fig. 2A). While successful perfusion of arterioles, venules, and capillaries were observed in cannulated microvascular networks, it is important to note a subset of capillaries and blind-ended blood-

filled capillaries were not perfused in some tissues (data not shown). The observation of nonperfused vessels is not unusual as vessels lacking perfusion are also commonly observed during intravital microscopy experiments.³² We speculate the apparent lack of perfusion in these vessels may be attributed to vessel blockage, collapse, or damage associated with tissue harvesting.

Evaluation of blood velocity profiles in capillary networks is important from a microvascular physiological point of view. Capillary blood flow regulates the supply of oxygen, nutrients, and waste products. Velocity also influences the relative wall shear stress in microvessels, which has been shown to regulate angiogenesis during microvascular remodeling.^{4,7}

In this study, we measured the velocity profiles in capillaries from four microvascular networks using fluorescent microbeads and live tissue imaging. By controlling peristaltic pump speed, we demonstrate a wide range of average capillary velocities ranging from 0.4 mm/s to 1.4 mm/s across four different microvascular networks (Fig. 3 and Supplementary Movie S1). These average velocity measurements are in the physiological range based on comparison with the literature using intravital microscopy to observe *in vivo* capillaries in rat mesentery tissue (0.96 mm/s–1.2 mm/s).^{33–35} The range of capillary velocities also reflects a heterogeneity characteristic of intact microvascular networks *in vivo*.³⁶

Fluorescent microbead velocities in larger arterioles (>28 μm) and venules (>38 μm) were too fast to capture

between frames making velocity measurements difficult to consistently replicate across the four microvascular networks (Supplementary Movie S2). However, arteriole and venule velocities and wall shear stresses were calculated for a subset of these vessel types downstream from feeding arterioles and draining venules (Supplementary Table S1). The average velocity measurements for these vessels were comparable to values from the literature.^{37–40} Future experiments will be needed to fully characterize the effects of input flow rate on vessel-specific velocities in the larger vessels.

The importance of wall shear stress in microvascular remodeling has been implicated in numerous processes, including vascular permeability, growth factor secretion, regulation of endothelial cell phenotype, and the onset of atherosclerosis.⁴¹ For example, Ueda *et al.* demonstrated that increased shear stress increased endothelial cell migration velocity on the surface of a collagen gel *in vitro*.⁴² In another study using an *in vivo* rabbit ear chamber, Ichioka *et al.* found that increased wall shear stress in microvessels improved wound healing angiogenesis.⁴³ In addition, Song and Munn demonstrated using a microfluidic device that a wall shear stress of 3 dyne/cm² reduced endothelial sprouting during vascular endothelial growth factor-induced angiogenesis.¹⁵

For this study, wall shear stresses were estimated from velocity measurements in perfused capillary networks assuming Poiseuille flow through a cylindrical tube using the following equation: $\tau = \mu 8(V_{\text{mean}}/D)$, where V_{mean} is the average velocity, d is the inner capillary diameter, and μ represents viscosity. Our estimations demonstrate a range of shear stresses from 2.6 dyne/cm² to 27.3 dyne/cm², which includes physiologically relevant values.³⁶

The importance of flow and shear stresses within the cultured microvascular networks is supported by the decreased microvascular network density in perfusion-cultured mesentery tissue compared to the static culture. Importantly, we found the amount of capillary sprouting between the Perfused and Static culture groups was comparable, indicating microvascular networks cultured with flow indeed underwent angiogenesis (Fig. 6). Considering the differences in vascular density between culture groups, our results suggest the lack of flow causes an enhanced rate of growth as increased density follows capillary sprouting.^{44,45} Other qualitative observations of perfusion effects during angiogenesis included decreased vessel tortuosity and the specific location and phenotype of capillary sprouts.

Invasive and introverting sprout phenotypes were evaluated in perfused and static-cultured microvascular networks. Invasive sprouts are defined by their outward growth into the avascular tissue region of mesentery tissue and introverting sprouts grow within central vascular regions of microvascular networks.²⁹ Analysis revealed that the percent invasive sprouts per total number of sprouts in perfused microvascular networks was increased compared to static-cultured tissues, indicating the presence of flow influences the outward growth of new capillary sprouts. Inversely, the percent introverting sprouts per total number of sprouts in static-cultured microvascular networks was increased, suggesting an enhanced growth rate demonstrated by the vascular density differences.

Altogether, our results support an effect of perfusion on network growth and motivate future studies to correlate

vessel-specific hemodynamics with localized sprouting dynamics (i.e., endothelial cell changes, formation of new anastomoses, evaluation of gene/protein expression for capillary sprout-specific phenotypes, and changes to the local stroma and ECM). In addition, this study motivates future experiments to evaluate how vessel-specific hemodynamics affect perivascular cell (i.e., smooth muscle and pericyte) coverage and phenotypic differentiation.

A limitation of our study was the difference in medium exchange between experimental groups. In the Perfused culture group, medium was continuously delivered through the lumens of microvascular networks over a 48-h time course. The bioreactor open-loop system required ~250 mL of medium delivered during culture compared to 10 mL for the Static culture group, where tissues were submerged in media and exchanged every 24 h. The medium amount difference between the Perfused and Static groups raises a question whether this contributed to the effects of angiogenesis.

To address this issue, we performed an additional experiment with a Media Sham experimental group to control for the amount of medium exchange associated with the open-loop perfusion protocol (Supplementary Fig. S3). The Media Sham group matched the amount of medium exchange with the Perfused group. Medium was exchanged by the 30G needle and at the same flow rate as the Perfused group. However, for the Media Sham group, the feeding arteriole was not cannulated. The Media Sham group displayed a comparable vascular density level compared to the Static control and an increased vascular density compared to the Perfused group. These results suggest that the attenuated angiogenic response for the cannulated Perfused group is indeed associated with microvascular network perfusion.

In summary, the results from this study establish a novel *ex vivo* microvascular network model that maintains the multicellular complexity of real tissue and incorporates vessel perfusion. We envision this experimental platform can help bridge the tissue engineering gap between current *in vitro* models and the *in vivo* microenvironment.

Acknowledgments

This work was supported by the National Institutes of Health under Award Number R01AG049821.

Disclosure Statement

No competing financial interests exist.

Supplementary Material

Supplementary Figure S1
 Supplementary Figure S2
 Supplementary Figure S3
 Supplementary Figure S4
 Supplementary Table S1
 Supplementary Movie S1
 Supplementary Movie S2

References

1. Akbari, E., Szychalski, G.B., and Song JW. Microfluidic approaches to the study of angiogenesis and the microcirculation. *Microcirculation* **24**, e12363, 2017.

2. Kelly-Goss, M.R., Sweat, R.S., Stapor, P.C., Peirce, S.M., and Murfee, W.L. Targeting pericytes for angiogenic therapies. *Microcirculation* **21**, 345, 2014.
3. Carmeliet, P. Mechanisms of angiogenesis and arteriogenesis. *Nat Med* **6**, 389, 2000.
4. Aranda-Espinoza, H. Implications of Fluid Shear Stress in Capillary Sprouting during Adult Microvascular Network Remodeling [Internet]. *Mechanobiol Endothel* 2015 [cited 2019 Apr 17]. Available from: www.taylorfrancis.com/
5. Davies, P.F. Flow-mediated endothelial mechanotransduction. *Physiol Rev* **75**, 519, 1995.
6. Helmke, B.P. Molecular control of cytoskeletal mechanics by hemodynamic forces. *Physiology* **20**, 43, 2005.
7. Skalak, T.C., and Price, R.J. The role of mechanical stresses in microvascular remodeling. *Microcirculation* **3**, 143, 1996.
8. Van Gieson Eric, J., Murfee Walter, L., Skalak Thomas, C., and Price Richard, J. Enhanced smooth muscle cell coverage of microvessels exposed to increased hemodynamic stresses in vivo. *Circ Res* **92**, 929, 2003.
9. Murfee, W.L., Van Gieson, E.J., Price, R.J., and Skalak, T.C. Cell proliferation in mesenteric microvascular network remodeling in response to elevated hemodynamic stress. *Ann Biomed Eng* **32**, 1662, 2004.
10. Zhou, Z., Pausch, F., Schlötzer-Schrehardt, U., Brachvogel, B., and Pöschl, E. Induction of initial steps of angiogenic differentiation and maturation of endothelial cells by pericytes in vitro and the role of collagen IV. *Histochem Cell Biol* **145**, 511, 2016.
11. Waters, J.P., Kluger, M.S., Graham, M., Chang, W.G., Bradley, J.R., and Pober, J.S. In vitro self-assembly of human pericyte-supported endothelial microvessels in three-dimensional coculture: a simple model for interrogating endothelial-pericyte interactions. *J Vasc Res* **50**, 324, 2013.
12. Wang, Y., Wang, Y., Zhou, Z., *et al.* Differential effects of sulforaphane in regulation of angiogenesis in a co-culture model of endothelial cells and pericytes. *Oncol Rep* **37**, 2905, 2017.
13. Moya, M.L., Hsu, Y.-H., Lee, A.P., Hughes, C.C.W., and George, S.C. In vitro perfused human capillary networks. *Tissue Eng Part C Methods* **19**, 730, 2013.
14. Osaki, T., Serrano, J.C., and Kamm, R.D. Cooperative effects of vascular angiogenesis and lymphangiogenesis. *Regen Eng Transl Med* **4**, 120, 2018.
15. Song, J.W., and Munn, L.L. Fluid forces control endothelial sprouting. *Proc Natl Acad Sci USA* **108**, 15342, 2011.
16. van Duinen, V., Zhu, D., Ramakers, C., van Zonneveld, A.J., Vulto, P., and Hankemeier, T. Perfused 3D angiogenic sprouting in a high-throughput in vitro platform. *Angiogenesis* **22**, 157, 2019.
17. Jeong, G.S., Han, S., Shin, Y., *et al.* Sprouting angiogenesis under a chemical gradient regulated by interactions with an endothelial monolayer in a microfluidic platform. *Anal Chem* **83**, 8454, 2011.
18. van der Meer, A.D., Vermeul, K., Poot, A.A., Feijen, J., and Vermes, I. A microfluidic wound-healing assay for quantifying endothelial cell migration. *Am J Physiol Heart Circ Physiol* **298**, H719, 2009.
19. Kaunas, R., Kang, H., and Bayless, K.J. Synergistic regulation of angiogenic sprouting by biochemical factors and wall shear stress. *Cell Mol Bioeng* **4**, 547, 2011.
20. Nicosia, R.F., and Ottinetti, A. Growth of microvessels in serum-free matrix culture of rat aorta. A quantitative assay of angiogenesis in vitro. *Lab Invest J Tech Methods Pathol* **63**, 115, 1990.
21. Murakami, T., Suzuma, K., Takagi, H., *et al.* Time-lapse imaging of vitreoretinal angiogenesis originating from both quiescent and mature vessels in a novel ex vivo system. *Invest Ophthalmol Vis Sci* **47**, 5529, 2006.
22. Sawamiphak, S., Ritter, M., and Acker-Palmer, A. Preparation of retinal explant cultures to study ex vivo tip endothelial cell responses. *Nat Protoc* **5**, 1659, 2010.
23. Norrby, K. In vivo models of angiogenesis. *J Cell Mol Med* **10**, 588, 2006.
24. Stapor, P.C., Azimi, M.S., Ahsan, T., and Murfee, W.L. An angiogenesis model for investigating multicellular interactions across intact microvascular networks. *Am J Physiol Heart Circ Physiol* **304**, H235, 2013.
25. Azimi, M.S., Motherwell, J.M., and Murfee, W.L. An ex vivo method for time-lapse imaging of cultured rat mesenteric microvascular networks. *J Vis Exp JoVE* **120**, 55183, 2017.
26. Azimi, M.S., Myers, L., Lacey, M., *et al.* An ex vivo model for anti-angiogenic drug testing on intact microvascular networks. *PLoS One* **10**, e0119227, 2015.
27. Motherwell, J.M., Azimi, M.S., Spicer, K., *et al.* Evaluation of arteriolar smooth muscle cell function in an ex vivo microvascular network model. *Sci Rep* **7**, 2195, 2017.
28. Motherwell, J.M., Anderson, C.R., and Murfee, W.L. Endothelial cell phenotypes are maintained during angiogenesis in cultured microvascular networks. *Sci Rep* **8**, 5887, 2018.
29. Anderson, C.R. Absence of OX-43 antigen expression in invasive capillary sprouts: identification of a capillary sprout-specific endothelial phenotype. *AJP Heart Circ Physiol* **286**, 346H, 2003.
30. Schindelin, J., Arganda-Carreras, I., Frise, E., *et al.* Fiji: an open-source platform for biological-image analysis. *Nat Methods* **9**, 676, 2012.
31. Maejima, D., Nagai, T., Bridenbaugh, E.A., Cromer, W.E., and Gashev, A.A. The position- and lymphatic lumen-controlled tissue chambers to study live lymphatic vessels and surrounding tissues ex vivo. *Lymphat Res Biol* **12**, 150, 2014.
32. Segal, S.S. Regulation of blood flow in the microcirculation. *Microcirculation* **12**, 33, 2005.
33. Richardson, D., Morton, R., and Howard, J. Effects of chronic nicotine administration on RBC velocity in mesenteric capillaries of the rat. *Blood Vessels* **14**, 318, 1977.
34. Jeong, J.H., Sugii, Y., Minamiyama, M., and Okamoto, K. Measurement of RBC deformation and velocity in capillaries in vivo. *Microvasc Res* **71**, 212, 2006.
35. Driessen, G.K., Heidtmann, H., and Schmid-Schönbein, H. Effect of hemodilution and hemoconcentration on red cell flow velocity in the capillaries of the rat mesentery. *Pflüg Arch* **380**, 1, 1979.
36. Pries, A.R., Reglin, B., and Secomb, T.W. Structural adaptation of microvascular networks: functional roles of adaptive responses. *Am J Physiol-Heart Circ Physiol* **281**, H1015, 2001.
37. Seki, J., and Lipowsky, H.H. In vivo and in vitro measurements of red cell velocity under epifluorescence microscopy. *Microvasc Res* **38**, 110, 1989.
38. Pries, A.R., Secomb, T.W., Gaehtgens, P., and Gross, J.F. Blood flow in microvascular networks. Experiments and simulation. *Circ Res* **67**, 826, 1990.
39. Pries Axel, R., and Secomb Timothy, W. Gaehtgens peter. Design principles of vascular beds. *Circ Res* **77**, 1017, 1995.

40. Pries, A.R., Secomb, T.W., and Gaehtgens, P. Structure and hemodynamics of microvascular networks: heterogeneity and correlations. *Am J Physiol Heart Circ Physiol* **269**, H1713, 1995.
41. Stapor, P.C., Wang, W., Murfee, W.L., and Khismatullin, D.B. The Distribution of fluid shear stresses in capillary sprouts. *Cardiovasc Eng Technol* **2**, 124, 2011.
42. Ueda, A., Koga, M., Ikeda, M., Kudo, S., and Tanishita, K. Effect of shear stress on microvessel network formation of endothelial cells with in vitro three-dimensional model. *Am J Physiol Heart Circ Physiol* **287**, H994, 2004.
43. Ichioka, S., Shibata, M., Kosaki, K., Sato, Y., Harii, K., and Kamiya, A. Effects of shear stress on wound-healing angiogenesis in the rabbit ear chamber. *J Surg Res* **72**, 29, 1997.
44. Murfee, W., Rehorn, M., Peirce, S., and Skalak, T. Perivascular cells along venules upregulate NG2 expression during microvascular remodeling. *Microcirculation* **13**, 261, 2006.
45. Stapor, P.C., and Murfee, W.L. Identification of class III β -tubulin as a marker of angiogenic perivascular cells. *Microvasc Res* **83**, 257, 2012.

Address correspondence to:

Walter L. Murfee, PhD

J. Crayton Pruitt Family Department

of Biomedical Engineering

University of Florida

1275 Center Drive

Gainesville, FL 32611

E-mail: wmurfee@bme.ufl.edu

Received: April 26, 2019

Accepted: July 2, 2019

Online Publication Date: August 2, 2019